# **Inorganic Chemistry**

pubs.acs.org/IC Article

# Two Distinct Cu(II)-V(IV) Superexchange Interactions with Similar Bond Angles in a Triangular "CuV<sub>2</sub>" Fragment

Yiran Wang,<sup>#</sup> Masayuki Fukuda,<sup>#</sup> Sergey Nikolaev,<sup>#</sup> Atsushi Miyake, Kent J. Griffith, Matthew L. Nisbet, Emily Hiralal, Romain Gautier, Brandon L. Fisher, Masashi Tokunaga, Masaki Azuma, and Kenneth R. Poeppelmeier\*



Cite This: Inorg. Chem. 2022, 61, 10234-10241



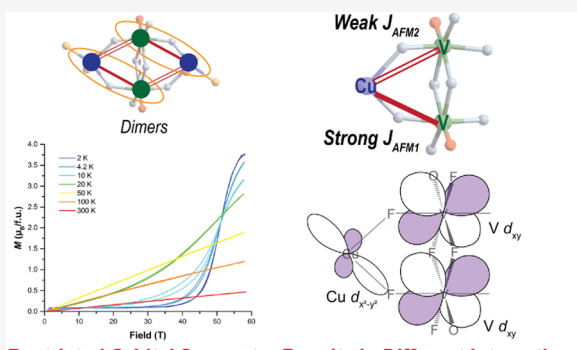
**ACCESS** 

Metrics & More

Article Recommendations

Supporting Information

**ABSTRACT:** The strength and sign of superexchange interactions are often predicted on the basis of the bond angles between magnetic ions, but complications may arise in situations with a nontrivial arrangement of the magnetic orbitals. We report on a novel molecular tetramer compound  $[Cu(H_2O)dmbpy]_2[V_2O_2F_8]$  (dmbpy = 4,4'-dimethyl-2,2'-bipyridyl) that is composed of triangular "CuV<sub>2</sub>" fragments and displays a spin gap behavior. By combining first-principles calculations and electronic models, we reveal that superexchange Cu–V interactions carry drastically different coupling strengths along two Cu–F–V pathways with comparable bond angles in the triangular "CuV<sub>2</sub>" fragment. Counterintuitively, their strong disparity is found to originate from the restricted symmetry of the half-filled Cu  $d_{x^2-y^2}$  orbital stabilized by the crystal field, leading to one dominating antiferromagnetic Cu–V



Restricted Orbital Symmetry Results in Different Interactions

coupling in each fragment. We revisit the magnetic properties of the reported spin-gapped chain compound  $[enH_2]Cu-(H_2O)_2[V_2O_2F_8]$  (en $H_2$  = ethylene diammonium) containing similar triangular " $CuV_2$ " fragments, and the magnetic behavior of the molecular tetramer and the chain compounds is rationalized as that of weakly coupled spin dimers and spin trimers, respectively. This work demonstrates that fundamentally different magnetic couplings can be observed between magnetic ions with similar bond angles in a single spin motif, thus providing a strategy to introduce various exchange interactions combined with low dimensionality in heterometallic Cu(II)-V(IV) compounds.

# **■ INTRODUCTION**

Anderson's kinetic exchange or superexchange interaction<sup>1,2</sup> is ubiquitous in insulating materials and magnetic molecules where two magnetic (M) ions are bridged by one or more nonmagnetic (N) ions. Many widely studied low-dimensional spin motifs are found to be mediated by superexchange interactions, including spin dimers in  $SrCu_2(BO_3)_{\mathcal{D}}^3$  spin ladders in  $SrCu_2O_3$ , Kagomé lattices in  $Cs_2Cu_2Cl_4$ ,  $[NH_4]_2[C_7H_{14}N][V_7O_6F_{18}]$ , and  $(CH_3NH_3)_2NaTi_3F_{12}$ , and many others where an unusual magnetic behavior can be expected from the reduced dimensionality and frustration.<sup>8–10</sup> With an increasing number of new magnetic systems, it is essential to accurately describe magnetic exchange couplings and understand their microscopic origin. In this regard, the Goodenough-Kanamori-Anderson (GKA) rules have been highly successful in providing a qualitative understanding of the magnetic properties in a wide range of materials.<sup>2,11–14</sup> In practice, however, important details of the orbital structure are discarded when the sign and strength of superexchange interactions are determined based only on the M-N-M bond angles following the GKA rules. As a result, some complications may arise when assigning exchange interactions

with bond angles in systems with a nontrivial spatial arrangement of the magnetic orbitals, such as in non-coplanar layouts and distorted geometries, <sup>13–17</sup> or in heterometallic materials, where unexpected exchange mechanisms may occur. <sup>18–21</sup>

Heterometallic Cu(II)–V(IV) compounds hold the potential for realizing various spin-1/2 motifs with low dimensionality and varying magnetic exchange interactions. A Cambridge Structural Database (CSD version 2020.1 from April 2020) search (see the details below) reveals that the magnetic properties of several one-atom-bridged Cu(II)–V(IV) compounds have been studied experimentally, where strong ferromagnetic (FM) and weak antiferromagnetic (AFM) Cu–V exchange interactions were reported based on magnetic data fitting. A classic example is strong ferromagnetic (FM)

Received: May 16, 2022 Published: June 23, 2022





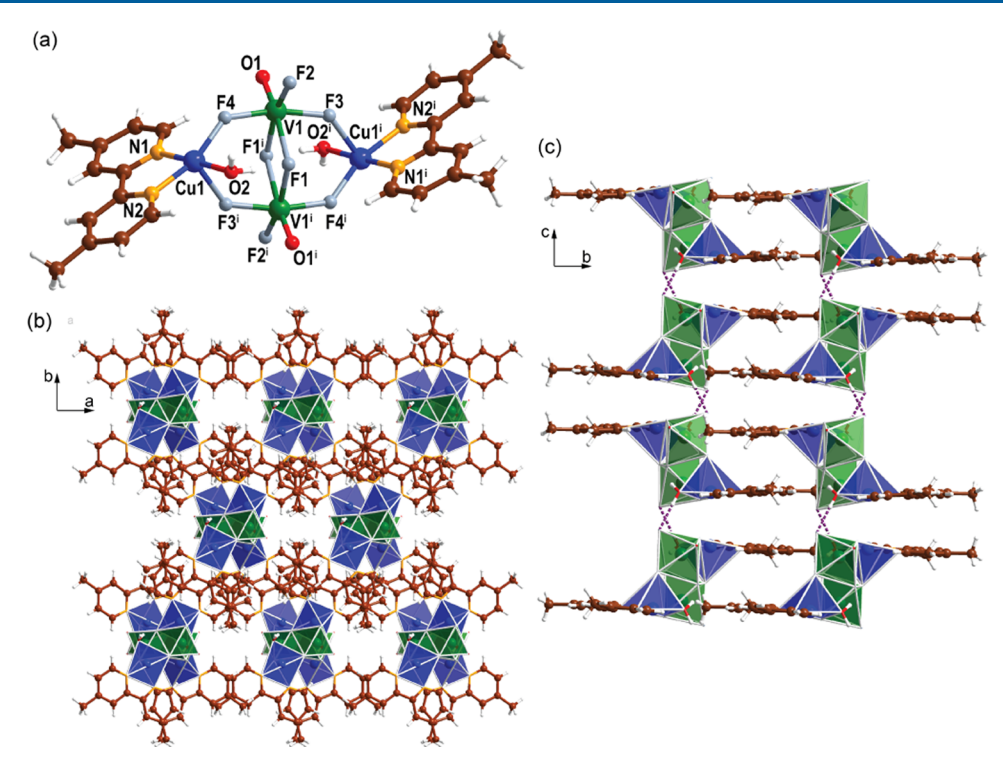


Figure 1. (a) Molecular and crystal structure of compound 1 along the (b) c-axis and (c) a-axis. Selected atoms are labeled. Blue, green, gray, red, orange, brown, and white spheres represent Cu, V, F, O, N, C, and H atoms, respectively. Blue and green octahedra represent copper-centered cations and vanadium-centered anions, respectively. The dashed line represents the hydrogen bond. [Symmetry code: (i) 1 - x, 1 - y, 1 - z].

coupling in a heterodinuclear copper(II)-vanadyl complex, demonstrated by Khan et al.,  $^{22,23}$  where the microscopic origin can be well rationalized by the GKA rules owing to the orthogonality of the magnetic orbitals.  $^{24}$  Nevertheless, strong AFM coupling that is essential for forming low-dimensional spin motifs has not been reported in heterometallic Cu(II)—V(IV) compounds.

In this study, we report on a new Cu(II)-V(IV) compound  $[Cu(H_2O)(dmbpy)]_2[V_2O_2F_8]$  (1) that features molecular tetramers composed of triangular "CuV2" fragments and displays a pronounced S = 0 spin-gapped behavior. By combining electronic and spin models with density functional theory (DFT) calculations, we demonstrate that, despite similar bond angles, Cu-V superexchange interactions carry drastically different coupling strengths along two Cu-F-V pathways in the triangular "CuV<sub>2</sub>" fragment, owing to the special orientation of the magnetic orbitals stabilized by the local atomic environment. To our knowledge, the dominating AFM Cu-V coupling in the triangular "CuV2" fragment displays the strongest AFM coupling among all of the reported Cu(II)-V(IV) compounds. This analysis is further applied to revisit the magnetic properties of the previously reported spingapped chain compound  $[enH_2]Cu(H_2O)_2[V_2O_2F_8]$  (enH<sub>2</sub> = ethylene diammonium, compound 2)<sup>25</sup> with the same triangular "CuV2" fragments. Based on the database analysis, superexchange interactions in compounds 1 and 2 are compared to other known Cu(II)-V(IV) systems, opening up an avenue for searching and realizing novel low-dimensional spin motifs in Cu(II)-V(IV) and other heterometallic compounds.

## RESULTS AND DISCUSSION

Synthesis, Structure, and Magnetic Properties of Compound 1. Dark green block crystals of compound 1 with

the formula  $[Cu(H_2O)(dmbpy)]_2[V_2O_2F_8]$  were synthesized through hydrothermal pouch methods. 26 Powder X-ray diffraction indicates the synthesis is bulk pure (Figure S1). Single-crystal X-ray diffraction reveals that compound 1 crystallizes in the monoclinic space group C2/c and features charge-neutral molecular tetramers where two [Cu(H<sub>2</sub>O)-(dmbpy)]<sup>2+</sup> fragments are bridged by a [V<sub>2</sub>O<sub>2</sub>F<sub>8</sub>]<sup>4-</sup> cluster (Figure 1a). The molecular tetramers pack into an extended 3D structure via  $\pi - \pi$  interactions between the dmbpy ligands and intermolecular hydrogen bonding O2-H2B···F2 along the c-axis (Figure 1b,c). The analysis of the bond valence sum (BVS) calculations<sup>27</sup> for compound 1 gives a valence of 1.81 and 3.93 for Cu and V (Table S2), respectively, suggesting the presence of Cu(II) and V(IV). The valence state and crystal structure were further supported by FTIR and NMR spectra (details in the Supporting Information).

To facilitate the analysis of magnetic properties in compound 1, we examined the coordination environments of V and Cu sites. The [V<sub>2</sub>O<sub>2</sub>F<sub>8</sub>]<sup>4-</sup> cluster is composed of two crystallographically equivalent heteroleptic [VOF<sub>4</sub>]<sup>2-</sup> octahedra with an out-of-center distortion and the distortion is stabilized by heteroanionic ligands. The shortest bond V1-O1 (1.6029(9) Å) in  $[V_2O_2F_8]^{4-}$  anions is trans to the longest bond V1-F1 (2.2267(7) Å). The V1-F bond distances on the equatorial positions of  $[V_2O_2F_8]^{4-}$  range from 1.9085(7) to 1.9860(7) Å. Moreover, the O1 atom displays low nucleophilicity from significant  $\pi$ -bonding to the V1 atom, resulting in high nucleophilicity in its trans F1 atom. Thus, the two  $[VOF_4]^{2^-}$  units are dimerized through F1, with the bond angle of  $V1-F1-V1^i$  being  $107.06(3)^\circ$ . Additionally, the [Cu(H<sub>2</sub>O)(dmbpy)]<sup>2+</sup> cations are linked to the [V<sub>2</sub>O<sub>2</sub>F<sub>8</sub>]<sup>4-</sup> clusters through F3 and F4 atoms, with the angles of Cu1-F3<sup>i</sup>-V1<sup>i</sup> and V1-F4-Cu1 being 131.67(4) and 136.25(4)°, respectively. Aside from F3 and F4¹, Cu1 is also

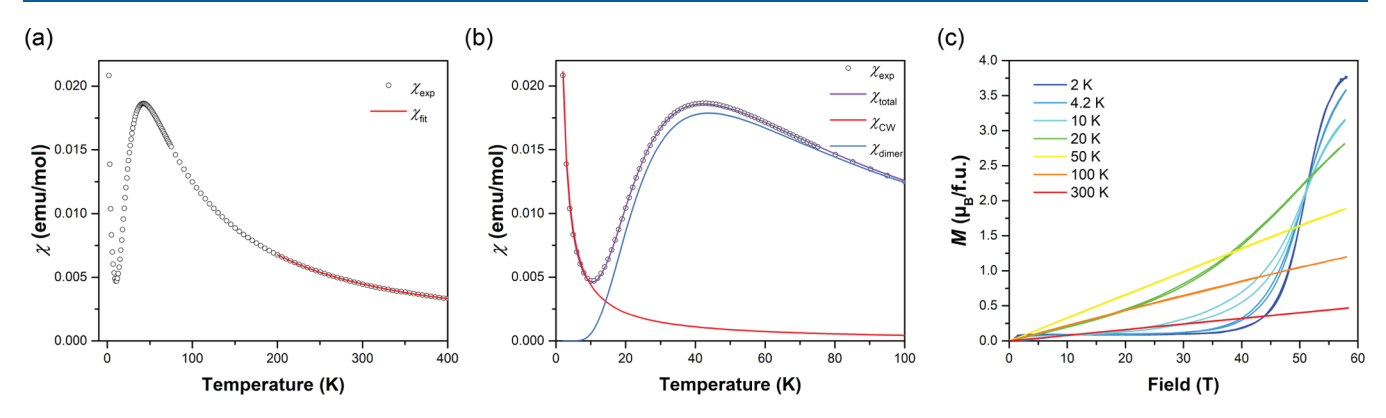


Figure 2. Magnetic data for compound 1. Variable-temperature magnetic susceptibility data under an external field of 0.1 T in the (a) high-temperature region and (b) low-temperature region. The results of fittings are plotted with solid lines and the experimental data are shown as open circles. (c) Magnetization curves as a function of magnetic field at various temperatures.

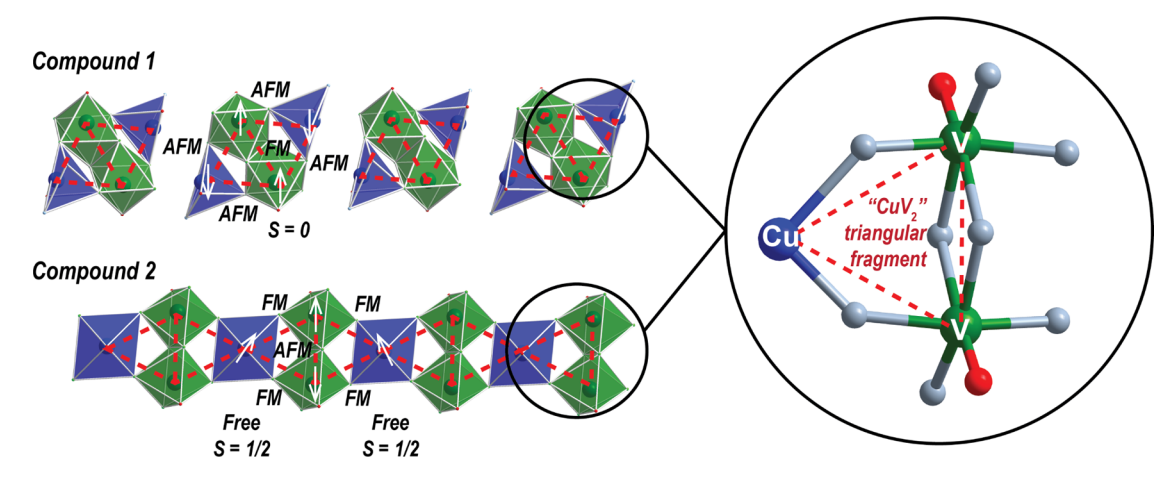


Figure 3. Structure comparison between compounds 1 and 2, and the illustration of triangular "CuV<sub>2</sub>" fragments. Green and blue polyhedra represent V-centered anions and Cu-centered cations, respectively. The red dashed line indicates the tentative superexchange pathways and spin models. The conflicted magnetic assignments between this work for compound 1 (upper) and the previous study for compound 2 (lower) are labeled.

coordinated to N1 and N2 from the dmbpy bidentate ligand and O2 from the water ligand. Cu1 is in a slightly distorted square pyramidal coordination environment, indicated by a small  $\tau_5$  parameter (0.24) given as  $\tau_5 = \frac{\beta - \alpha}{60^\circ}$  where  $\beta$  and  $\alpha$  are the largest and the second largest bond angles in the polyhedron. The bond distances in the copper polyhedron are 1.9858(9), 1.9853(9), 1.9706(8), 2.1487(7), and 1.9358(7) Å for Cu1–N1, Cu1–N2, Cu1–O2, Cu1–F3<sup>i</sup>, and Cu1–F4, respectively. Notably, the Cu1–F3<sup>i</sup> bond is significantly longer than the other Cu1 coordinate bonds owing to the pyramidal coordination of Cu<sup>2+</sup> ions.

To probe the magnetic properties of compound 1, variable-temperature magnetic susceptibility data were collected under an external field of 0.1 T (Figure 2). The magnetic susceptibility is found to exhibit Curie—Weiss temperature dependence from 200 to 400 K

$$\chi(T) = \chi_0 + C/(T - \theta)$$

where  $\chi_0$  is a temperature-independent susceptibility term, C is the Curie constant, and  $\theta$  is the Weiss temperature. Data fitting gives  $\chi_0 = -1.1(5) \times 10^{-4}$  emu/mol, C = 1.37(3) emu K/mol, and  $\theta = 0.9(27)$  K (Figure 2a). The calculated value of C agrees with a theoretical value of 1.5 emu K/mol that is expected for two Cu(II) and two V(IV) ions. Also,  $1/\chi$  is

approximately proportional to temperature above 100 K in Figure S4, which supports the paramagnetic behavior of compound 1 in the high-temperature range.

In the temperature range of 10-50 K, the magnetic susceptibility of compound 1 starts to deviate from the Curie–Weiss law and decreases toward a projected value of  $\chi(0 \text{ K}) = 0 \text{ emu/mol}$ , indicating the formation of a nonmagnetic spin singlet state. At 10 K, there is another inflection point, below which the magnetic susceptibility increases again, suggesting the presence of free spins. To model the behavior in this complex, the magnetic susceptibility of compound 1 below 100 K was fitted to the following equation

$$\chi_{\text{total}} = \chi_0 + \chi_{\text{CW}} + \chi_{\text{dimer}}$$
  
=  $\chi_0 + C_1/(T - \theta) + 3(C_2/T)/(3 + e^{\Delta/T})$ 

where  $\chi_0$  is the temperature-independent term,  $\chi_{\rm CW}$  is the contribution from the free spins following the Curie–Weiss law with a Curie constant of  $C_1$  and a Weiss constant of  $\theta$ ;  $\chi_{\rm dimer}$  is the term associated with spin dimers, where  $\Delta$  is a spin gap from the singlet ground state to the triplet excited state, and  $C_2$  is the corresponding Curie constant. With the parameters being varied freely, the fitting gives  $\chi_0 = -3.0(3) \times 10^{-4}$  emu/mol,  $C_1 = 4.44(4) \times 10^{-2}$  emu K/mol,  $\theta = -3.0(3)$ 

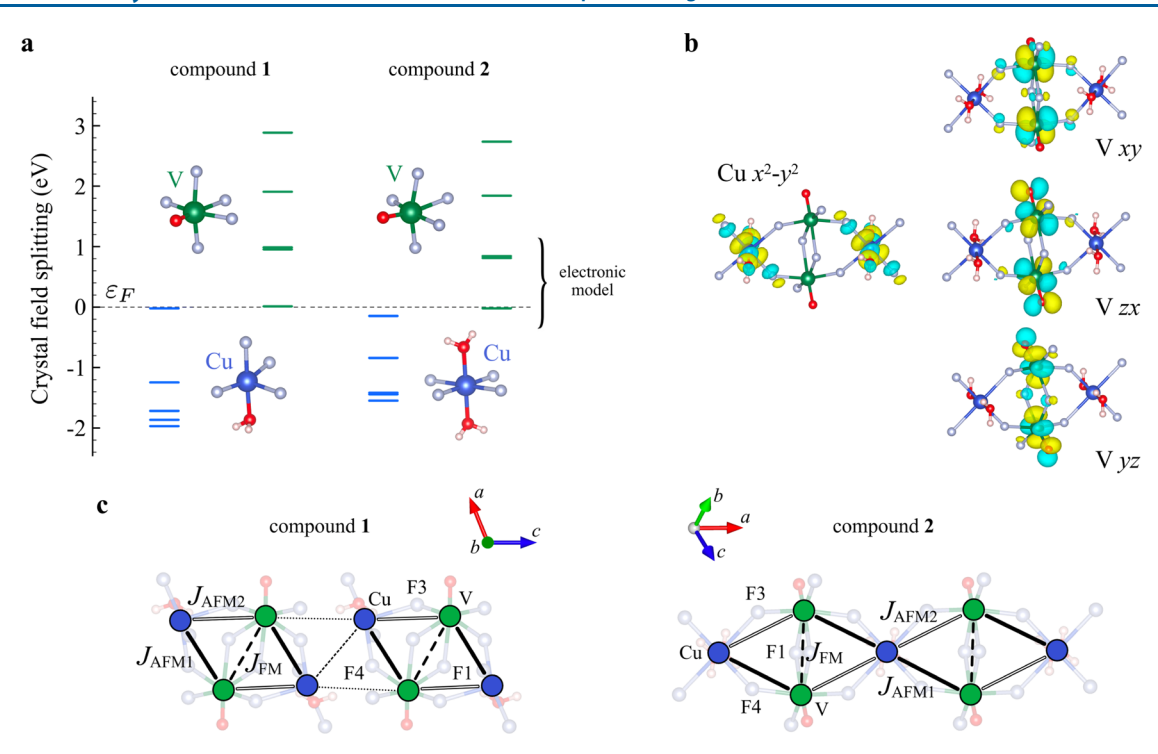


Figure 4. (a) Crystal-field splitting of the 3d electrons at Cu (blue levels) and V (green levels) sites for compounds 1 (left) and 2 (right). Electronic states used for constructing the minimal electronic model are shown with figure brackets. (b) Wannier functions corresponding to the Cu  $d_{x^2-y^2}$  and V  $t_{2g}$  states (arbitrarily named as  $d_{xy}$ ,  $d_{zx}$ ,  $d_{yz}$ ) as constructed for compound 2. The same set of Wannier functions is employed for compound 1. (c) Schematic of the spin models in compounds 1 (left) and 2 (right). Thick black  $(J_{AFM1})$ , hollow  $(J_{AFM2})$ , and thick dashed  $(J_{FM})$  lines denote the strong and weak AFM  $J_{Cu-V}$  and the weak FM  $J_{V-V}$  interactions, respectively. Thin dotted lines in compound 1 represent weak AFM couplings between neighboring tetramers.

-0.10(2) K,  $C_2 = 2.081(4)$  emu K/mol, and  $\Delta = 70.24(4)$  K (Figure 2b). The small  $C_1$  value (<5% spin contribution) implies the presence of free spins that likely originate from a small number of defects or a very small amount of another phase, which was undetectable in the XRD experiment. The  $C_2$  value is about 1.4 times larger than expected (1.5 emu K/mol); nevertheless, the data can be reproduced well with the model adopted in this study, demonstrating the existence of a spin gap.

To further investigate the spin gap in compound 1, variable field magnetization data were collected under a pulsed high magnetic field up to 58 T (Figure 2c). At 2 K, the magnetization at low magnetic fields remains close to 0  $\mu_{\rm B}$ , indicating a nonmagnetic singlet ground state, in agreement with the susceptibility data. As the applied magnetic field increases, the sample magnetization shows a sudden increase at around 40 T, revealing a transition from the singlet ground state to the triplet excited state. The magnetization saturates at 3.8  $\mu_{\rm B}$  at 58 T, close to the value of 4  $\mu_{\rm B}$  that is expected for a full magnetic moment of the tetramer with two Cu(II) and two V(IV) ions. The magnitude of the spin gap estimated from the crossover field of 45 T is 57.6 K. This is slightly smaller than the obtained value from the susceptibility data fitting at low temperatures (70.24 K). Similar trends have been reported in previous studies on spin singlet compounds. 25,31 Considering the presence of the spin gap, we tentatively assumed the formation of AFM spin tetramers in compound 1 as illustrated in Figure 3.

Conflicted Superexchange Assignments from a Previous Study. The triangular "CuV<sub>2</sub>" fragments found in compound 1 were previously reported in another crystal  $[enH_2]Cu(H_2O)_2[V_2O_2F_8]$ , namely, compound 2.<sup>25</sup> Unlike

the molecular-like structure in 1, compound 2 features onedimensional chain structures as a result of a higher Cu coordination number (Figure 3). In compound 1, Cu atoms are five-coordinated, leading to segregated molecular tetramers, whereas in compound 2, Cu atoms are six-coordinated, allowing "CuV<sub>2</sub>" fragments to connect into chains through *cis*-corner-sharing metal-centered octahedra. Although these compounds have different extended structures, their basic building units formed by triangular "CuV<sub>2</sub>" fragments show highly similar bonding characteristics (Table S3).

Given their structural similarities, comparable magnetic coupling between V-V and Cu-V can be expected to arise in both compounds. According to the previous study, the magnetic behavior of compound 2 was ascribed to AFM V-V and FM Cu-V exchange interactions based on the bond angles with adjacent nonmagnetic ions.<sup>25</sup> The spin gap behavior in compound 2 was rationalized by assuming the formation of a V-V spin dimer and one free Cu(II) spin, being effectively decoupled due to magnetic frustration (as shown in Figure 3). Consequently, the observed magnetization featuring two plateau states was ascribed to a quick saturation to S = 1/2by a free spin at a magnetic field below 10 T and then to S = 3/2 at high magnetic fields (>38 T) when the dimer singlet state is destroyed.<sup>25</sup> Following this analysis, it is reasonable to assume that if a similar magnetic scenario is held in compound 1, each tetramer would contain two free Cu spins, resulting in an S = 1 magnetic state at low magnetic fields. This would contradict the observed S = 0 nonmagnetic behavior, thus being inefficient to explain their distinct magnetic properties and questioning the previously assigned magnetic scenario. It is evident that magnetic exchange interactions mediated in the isostructural triangular "CuV2" fragments of compounds 1 and

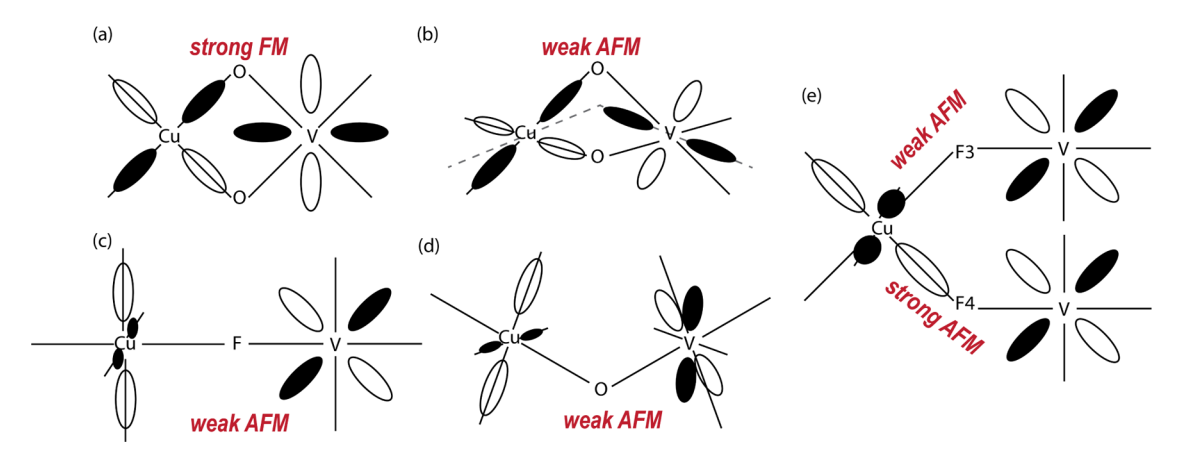


Figure 5. Magnetic mechanisms in (a) BIGFAY, DAKROW, PUSJOC, and SEJPON, (b) RAXTOB (the gray lines indicate the non-coplanar fact), (c) UXOZEO02, (d) CuVOF<sub>4</sub>(H<sub>2</sub>O)<sub>6</sub>·H<sub>2</sub>O, (e) Cu-F3-V and Cu-F4-V pathways of the triangular "CuV<sub>2</sub>" fragments (this work).

2 should yield comparable spin models and thus have to be revisited to capture the magnetic behavior of both the systems.

Electronic and Spin Models for Compounds 1 and 2. To provide a microscopic description of the magnetic properties in both compounds 1 and 2, we constructed electronic Hubbard-type models based on first-principles calculations that take into account all necessary ingredients to specify their magnetic behavior. From the calculated electronic structures (Figure S5), one can see that the states near the Fermi level are primarily formed by the Cu and V 3d states occupying one hole and one electron, respectively. Owing to their large crystal-field splitting, a minimal multiorbital Hubbard model for both the compounds can be formulated in the basis of Wannier functions corresponding to the Cu  $3d_{x^2-y^2}$  and V  $t_{2g}$  ( $3d_{xy}$ ,  $3d_{zx}$ ,  $3d_{yz}$ ) states, as shown in Figure 4b

$$\mathcal{H} = \mathcal{H}_{\mathrm{CF}} + \sum_{\substack{ij\\mm',\sigma}} t_{i,j}^{mm} c_{im}^{\dagger\sigma} c_{jm}^{\sigma}, + \mathcal{H}_{U}^{\mathrm{Cu}} + \mathcal{H}_{U}^{\mathrm{V}}$$

where the first term stands for the crystal-field splitting, the second term corresponds to kinetic energy, and the last two terms are the on-site Coulombic interactions. The details on model construction and the resulting model parameters are given in the Supporting Information. It can be seen that both systems fall into a strongly correlated regime with  $t \ll U$ , that will open a gap at the Fermi level and lead to an insulating state. Hopping parameters between Cu and V within the "CuV<sub>2</sub>" fragment are found to be highly asymmetric due to a specific spatial orientation of the half-filled Cu  $3d_{r^2-v^2}$  orbital stabilized by the crystal field (as illustrated in Figure 4b). The latter leads to disproportionate orbital overlap along two Cu-F3-V and Cu-F4-V paths, despite their similar bond angles. Importantly, the orientation of the half-filled Cu  $3d_{r^2-v^2}$  orbital stabilized by the crystal field is the same in both compounds regardless of their different coordination and chemical environment. On the other hand, hopping parameters along the V-F1-V path prevail predominantly between unoccupied orbitals that in turn will favor FM coupling according to the GKA rules.

The derived Hubbard models can further be mapped onto the isotropic spin Heisenberg models using the theory of superexchange starting from the single occupied Cu  $d_{x^2-y^2}$  and V  $t_{2g}$  orbitals (details in the Supporting Information). The calculated isotropic exchange parameters are  $J_{\rm FM} \equiv J_{\rm V-F1-V} =$ 

-0.16 and -0.39 meV,  $J_{\rm AFM1} \equiv J_{\rm Cu-F4-V} = 7.39$  and 6.84 meV, and  $J_{\rm AFM2} \equiv J_{\rm Cu-F3-V} = 0.29$  and 0.25 meV for compounds 1 and 2, respectively. The Cu–Cu exchange interactions for both compounds as well as intercluster exchange parameters for compound 1 are weakly AFM, owing to the small magnitude of the hopping parameters and can be discarded from the analysis. Our results demonstrate that the magnetic behavior of both compounds is governed by strong AFM Cu–F4–V coupling that significantly outweighs adjacent AFM Cu–F3–V and FM V–F1–V interactions in the "CuV<sub>2</sub>" fragment. In the previous study, all exchange interactions were erroneously found to have the opposite sign. <sup>25</sup>

The calculated magnetization as a function of magnetic field and temperature is shown in Figure S7, whose qualitative behavior is in excellent agreement with the experiment for both systems. The calculated spin gap for compound 2 is found to be  $\sim$ 120 K, which is larger than the previously reported value of 60 K but can further be reduced by extending the electronic model and including other exchange interactions. The calculated value of the saturation magnetic field of  $\sim$ 65 T (assuming g=2) for compound 1 is in good agreement with the experimental value of 58 T.

Thus, one can see that the magnetic properties of compound 1 directly follow those of a simple spin dimer, while the quasione-dimensional chains in compound 2 can be regarded as a chain of weakly coupled linear spin-1/2 trimers  $J_{AFM1}$   $S_1 \cdot S_2$  +  $J_{AFM1}$   $S_2 \cdot S_3$ , where only two pairs of neighboring spins are antiferromagnetically coupled (as schematically shown in Figure 5c). Other examples of spin trimers were reported in compounds  $A_3Cu_3(PO_4)_4$  (A = Ca, Sr, Pb),<sup>32</sup> ( $C_5H_{11}NO_2)_2$ ·  $3CuCl_2$ ·  $2H_2O_7$ <sup>33</sup> and  $Cu_3(P_2O_6OH)_2$ .<sup>34</sup> From the energy diagram in Figure S8, it follows that in the absence of a magnetic field, the ground state of the spin-1/2 trimer is double degenerate and given as a superposition of two S = 0 $\frac{1}{\sqrt{6}}(|\uparrow\uparrow\downarrow\rangle - 2|\uparrow\downarrow\uparrow\rangle + |\downarrow\uparrow\uparrow\rangle)$  $\frac{1}{\sqrt{6}}(|\uparrow\downarrow\downarrow\rangle-2|\downarrow\uparrow\downarrow\rangle+|\downarrow\downarrow\uparrow\rangle)$ . Upon applying a magnetic field, the degeneracy is lifted, and at a critical field  $h = \frac{3J_{AFM1}}{2}$ , the S = 1/2 configuration  $\frac{1}{\sqrt{6}}(|\uparrow \uparrow \downarrow \rangle - 2|\uparrow \downarrow \uparrow \rangle + |\downarrow \uparrow \uparrow \rangle)$ further changes to the fully polarized state  $|\uparrow\uparrow\uparrow\rangle$  with S=3/2. It is worth noting that the revisited spin model for compound 2 fits well and explains the temperature dependence of the

reported magnetic susceptibility and spin gap behavior (see the Supporting Information).

Varied Cu(II)-V(IV) Superexchange Mechanisms from Different Spatial Arrangements of the Magnetic Orbitals. As demonstrated by our calculations, both the previously reported magnetic assignment for compound 2 and tentative magnetic assignment for compound 1 are found to be inadequate for the triangular "CuV<sub>2</sub>" fragment. Namely, the two Cu(II)-V(IV) superexchange pathways in the fragment that were considered to be equivalent in the previous study turn out to be drastically different, with substantially disproportionate coupling strengths. This result is essentially not intuitive, considering the similar bond angles in the Cu-F3-V and Cu-F4-V pathways of the triangular "CuV<sub>2</sub>" fragment (see Figure S9).

Apart from the two systems considered in this work, there are several other heterometallic Cu(II)-V(IV) compounds with reported strong FM and weak AFM interactions. In the search in Cambridge Structural Database (CSD version 2020.1 from April 2020), we found 522 compounds containing both Cu and V (see Figure S10 and spreadsheet in the Supporting Information). Among these systems, 164 compounds contain at least one Cu(II) and one V(IV) atom, with 99 of them having Cu and V connected through a one-atom bridge, which can potentially mediate superexchange interactions (transition metals in some compounds were reported to have ambiguous or mixed valence states). Nevertheless, among these 99 oneatom-bridged compounds, only eight compounds (CSD REFCODE: BIGFAY;<sup>23</sup> DAKROW;<sup>35</sup> PUSJOC;<sup>36</sup> SEJPON;<sup>37</sup> RAXTOB;<sup>38</sup> UXOZEO02;<sup>39</sup> RAGCAE01;<sup>40</sup> and XAKXUD<sup>41</sup>) have been reported experimentally with the available magnetic data fitted into spin models (see Table S4, including the study of compound 2). 23,25,35-41 In addition to the two compounds from the present study, only one compound is found to be bridged by an F atom, while the other seven compounds are bridged by an O atom.

Among the eight studied compounds, four compounds (BIGFAY;<sup>23</sup> DAKROW;<sup>35</sup> PUSJOC;<sup>36</sup> SEJPON<sup>37</sup>) were reported to exhibit strong FM Cu(II)-V(IV) coupling and contain Cu-V clusters in which Cu is double-bridged to V through O atoms, all residing in the same plane (Figure 5a). Kahn et al. have attributed strong FM superexchange interactions to the orthogonality of the magnetic Cu  $d_{x^2-y^2}$  and V  $d_{xy}$  orbitals.<sup>23,37</sup> Having different symmetries with respect to the mirror plane of the complex, their overlap cancels out, suppressing the AFM contribution and stabilizing strong FM coupling between Cu(II) and V(IV). In the remaining four compounds, RAXTOB<sup>38</sup> also contains Cu and V double-bridged by O atoms, which are not coplanar, with the dihedral angle of the planes containing Cu  $d_{x^2-y^2}$  and V  $d_{xy}$ orbitals being 135.4° (Figure 5b). In this case, data fitting gives a weak Cu-V AFM coupling, which was ascribed to the noncoplanarity of the magnetic orbitals, allowing for their small overlap.

In contrast to the systems above, UXOZEO02<sup>39</sup> has an entirely different connectivity in which Cu is connected to V through a single F bridge, and the Cu–F–V path forms a linear 180° bond (Figure 5c). However, lateral overlap of the Cu  $d_{x^2-y^2}$  and V  $d_{xy}$  orbitals is rather small, leading to a nearly zero AFM superexchange coupling with a fitting value of J=0.04 meV. As for the last two compounds RAGCAE01<sup>40</sup> and XAKXUD, <sup>41</sup> the magnetic data were fitted into a Heisenberg mixed-dimer model with weak AFM couplings, but no further

discussion was provided on their mechanism. Apart from the aforementioned scenarios, a recent study on the magnetic properties of  $\text{CuVOF}_4(\text{H}_2\text{O})_6\text{·H}_2\text{O}$  affords another unusual situation (Figure 5d).  $^{42,43}$  In this compound, Cu is connected to V through a O bridge with a bond angle of 142.88° and the Cu(II)-V(IV) coupling is fitted into a dimer model with the fitted value of 1.81 meV. First-principles calculations reveal that the magnetic orbitals reside in the Jahn–Teller plane and a significant spin density at the bridging O atom leads to a quantum disordered state at low magnetic fields.

As a new example, superexchange interactions in compounds 1 and 2 are mediated by another strikingly different scenario. The crystal field of Cu(II) ions fixes the lobes of the half-filled Cu  $d_{x^2-y^2}$  orbital to align along the Cu-F4 direction and be perpendicular to the Cu-F3 bond (Figure 5e), which is similar in both compounds despite their different coordination and chemical environments. As a result, the Cu-F4  $\sigma$  bonding is found to be much stronger, owing to direct orbital overlap, than the one along the Cu-F3, despite their similar bond connectivity in the triangular "CuV2" fragment. Moreover, unlike the scenario in Figure 5a,b, the bond angle and the dihedral angle of the planes containing Cu  $d_{x^2-y^2}$  and V  $d_{xy}$ orbitals in the Cu-F4-V pathway avoid the special symmetry to suppress the AFM contribution. Thus, the magnetic coupling via the Cu-F4-V pathway displays the strongest AFM coupling strength among all of the reported Cu(II)-V(IV) compounds. Summing up, the versatile magnetic orbital arrangements in heterometallic Cu(II)-V(IV) coupling offer six different magnetic mechanisms within 11 compounds and the diverse magnetic interactions between Cu(II)-V(IV) ions can be manipulated by coordination geometries and ligand choice. In addition, the microscopic scenario realized in the triangular "CuV2" fragment offers an approach to maximize AFM interactions, providing opportunities to realize emergent AFM spin motifs with Cu(II)-V(IV) compounds.

# CONCLUSIONS

Through the unique triangular " $CuV_2$ " fragment, this study has demonstrated that distinct superexchange interactions can exist in a single spin motif in the presence of similar bond angles, thus emphasizing the importance of the orbital structure in the case of a nontrivial arrangement of magnetic ions. Based on DFT calculations and electronic models, a microscopic description of the observed spin gap behavior in the newly synthesized compound 1 and previously reported compound 2 has been provided. Two essentially distinct AFM Cu-V couplings in the " $CuV_2$ " fragment are found to originate from a specific orientation of the magnetic orbitals stabilized by the crystal field. This work offers another perspective on searching for new low-dimensional magnetic systems and shows that heterometallic materials can be regarded as a promising platform for realizing various spin motifs.

# ASSOCIATED CONTENT

# Supporting Information

The Supporting Information is available free of charge at https://pubs.acs.org/doi/10.1021/acs.inorgchem.2c01691.

Additional experimental details, characterization data, and CSD search; crystallographic data for compound 1 (PDF)

#### **Accession Codes**

CCDC 2159103 contains the supplementary crystallographic data for this paper. These data can be obtained free of charge via <a href="https://www.ccdc.cam.ac.uk/data\_request/cif">www.ccdc.cam.ac.uk/data\_request/cif</a>, or by emailing data\_request@ccdc.cam.ac.uk, or by contacting The Cambridge Crystallographic Data Centre, 12 Union Road, Cambridge CB2 1EZ, UK; fax: +44 1223 336033.

CCDC 2159103 contains the supplementary crystallographic data for this paper. These data can be obtained free of charge via www.ccdc.cam.ac.uk/data\_request/cif, or by emailing data\_request@ccdc.cam.ac.uk, or by contacting The Cambridge Crystallographic Data Centre, 12 Union Road, Cambridge CB2 1EZ, U.K.; fax: +44 1223 336033.

## AUTHOR INFORMATION

## **Corresponding Author**

Kenneth R. Poeppelmeier — Department of Chemistry, Northwestern University, Evanston, Illinois 60208, United States; orcid.org/0000-0003-1655-9127; Email: krp@northwestern.edu

#### **Authors**

Yiran Wang — Department of Chemistry, Northwestern University, Evanston, Illinois 60208, United States; orcid.org/0000-0002-3642-2294

Masayuki Fukuda — Materials and Structures Laboratory, Tokyo Institute of Technology, Yokohama 226-8503, Japan; o orcid.org/0000-0002-3153-9602

Sergey Nikolaev — Materials and Structures Laboratory, Tokyo Institute of Technology, Yokohama 226-8503, Japan Atsushi Miyake — The Institute for Solid State Physics, The University of Tokyo, Kashiwa, Chiba 277-8581, Japan

Kent J. Griffith – Department of Chemistry, Northwestern University, Evanston, Illinois 60208, United States; orcid.org/0000-0002-8096-906X

Matthew L. Nisbet – Department of Chemistry, Northwestern University, Evanston, Illinois 60208, United States

Emily Hiralal – Department of Chemistry, Northwestern University, Evanston, Illinois 60208, United States

Romain Gautier – Institut des Matériaux Jean Rouxel (IMN), Université de Nantes, CNRS, F-44000 Nantes cedex 3, France

Brandon L. Fisher — Nanoscale Science and Technology Division, Argonne National Laboratory, Lemont, Illinois 60439, United States

Masashi Tokunaga — The Institute for Solid State Physics, The University of Tokyo, Kashiwa, Chiba 277-8581, Japan; orcid.org/0000-0002-1401-9381

Masaki Azuma — Materials and Structures Laboratory, Tokyo Institute of Technology, Yokohama 226-8503, Japan;
o orcid.org/0000-0002-8378-321X

Complete contact information is available at: https://pubs.acs.org/10.1021/acs.inorgchem.2c01691

# **Author Contributions**

<sup>#</sup>Y.W., M.F., and S.N. contributed equally to this work.

The authors declare no competing financial interest.

## ACKNOWLEDGMENTS

This work was supported by funding from the National Science Foundation (DMR-1904701) and Grants-in-Aid for

Scientific Research, JP18H05208, JP19H05625, and JP21K18891 from the Japan Society for the Promotion of Science (JSPS). Y.W. acknowledge funding from the MRSEC program of the National Science Foundation (DMR-1720139) at the Materials Research Center of Northwestern University. K.J.G. acknowledges funding from the Joint Center for Energy Storage Research (ICESR), an Energy Innovation Hub funded by the US Department of Energy, Office of Science, Basic Energy Sciences. Single-crystal and powder X-ray diffraction data, FTIR spectra, and solid-state NMR spectra were acquired at IMSERC at Northwestern University, which has received support from the Soft and Hybrid Nanotechnology Experimental (SHyNE) Resource (NSF ECCS-1542205), the State of Illinois, the International Institute for Nanotechnology (IIN), and the National Science Foundation (DMR-0521267). Use of the Center for Nanoscale Materials, a DOE Office of Science User Facility, was supported by the U.S. Department of Energy, Office of Science, Office of Basic Energy Sciences, under Contract No. DE-AC02-06CH11357. The authors thank Dr. J. C. Hancock, Mr. I. L. Peczak, and Mr. A. D. Sample for helpful discussions and Ms. C. Stern for experimental assistance.

# REFERENCES

- (1) Anderson, P. W. Antiferromagnetism. Theory of Superexchange Interaction. *Phys. Rev.* **1950**, *79*, 350–356.
- (2) Goodenough, J. B. Theory of the Role of Covalence in the Perovskite-Type Manganites [La, M(II)]MnO<sub>3</sub>. *Phys. Rev.* **1955**, *100*, 564–573.
- (3) Kageyama, H.; Yoshimura, K.; Stern, R.; Mushnikov, N. V.; Onizuka, K.; Kato, M.; Kosuge, K.; Slichter, C. P.; Goto, T.; Ueda, Y. Exact Dimer Ground State and Quantized Magnetization Plateaus in the Two-Dimensional Spin System SrCu<sub>2</sub>(BO<sub>3</sub>)<sub>2</sub>. *Phys. Rev. Lett.* **1999**, 82, 3168–3171.
- (4) Azuma, M.; Hiroi, Z.; Takano, M.; Ishida, K.; Kitaoka, Y. Observation of a Spin Gap in SrCu<sub>2</sub>(BO<sub>3</sub>)<sub>2</sub> Comprising Spin-1/2 Quasi-1D Two-Leg Ladders. *Phys. Rev. Lett.* **1994**, *73*, 3463–3466.
- (5) Coldea, R.; Tennant, D. A.; Tsvelik, A. M.; Tylczynski, Z. Experimental Realization of a 2D Fractional Quantum Spin Liquid. *Phys. Rev. Lett.* **2001**, *86*, 1335–1338.
- (6) Aidoudi, F. H.; Aldous, D. W.; Goff, R. J.; Slawin, A. M. Z.; Attfield, J. P.; Morris, R. E.; Lightfoot, P. An Ionothermally Prepared S=1/2 Vanadium Oxyfluoride Kagome Lattice. *Nat. Chem.* **2011**, 3, 801–806.
- (7) Jiang, N.; Ramanathan, A.; Bacsa, J.; La Pierre, H. S. Synthesis of a D1-Titanium Fluoride Kagome Lattice Antiferromagnet. *Nat. Chem.* **2020**, *12*, *691–696*.
- (8) Katsumata, K. Low-Dimensional Magnetic Materials. Curr. Opin. Solid State Mater. Sci. 1997, 2, 226–230.
- (9) Vasiliev, A.; Volkova, O.; Zvereva, E.; Markina, M. Milestones of Low-D Quantum Magnetism. *Npj Quantum Mater.* **2018**, *3*, 18.
- (10) Balents, L. Spin Liquids in Frustrated Magnets. *Nature* 2010, 464, 199-208.
- (11) Goodenough, J. B. An Interpretation of the Magnetic Properties of the Perovskite-Type Mixed Crystals  $La_{1-x}Sr_xCoO_{3-\lambda}$ . J. Phys. Chem. Solids 1958, 6, 287–297.
- (12) Kanamori, J. Superexchange Interaction and Symmetry Properties of Electron Orbitals. J. Phys. Chem. Solids 1959, 10, 87–98.
- (13) Kanamori, J. Crystal Distortion in Magnetic Compounds. J. Appl. Phys. 1960, 31, S14–S23.
- (14) Geertsma, W.; Khomskii, D. Influence of Side Groups on 90° Superexchange: A Modification of the Goodenough-Kanamori-Anderson Rules. *Phys. Rev. B* **1996**, *54*, 3011–3014.
- (15) Lin, L.-F.; Zhang, Y.; Alvarez, G.; Moreo, A.; Dagotto, E. Origin of Insulating Ferromagnetism in Iron Oxychalcogenide Ce<sub>2</sub>O<sub>2</sub>FeSe<sub>2</sub>. *Phys. Rev. Lett.* **2021**, *127*, No. 077204.

- (16) Dabrowski, B.; Kolesnik, S.; Baszczuk, A.; Chmaissem, O.; Maxwell, T.; Mais, J. Structural, Transport, and Magnetic Properties of RMnO<sub>3</sub> Perovskites (R=La, Pr, Nd, Sm, 153Eu, Dy). *J. Solid State Chem.* **2005**, *178*, 629–637.
- (17) Blake, G. R.; Palstra, T. T. M.; Ren, Y.; Nugroho, A. A.; Menovsky, A. A. Transition between Orbital Orderings in YVO<sub>3</sub>. *Phys. Rev. Lett.* **2001**, *87*, No. 245501.
- (18) Azuma, M.; Takata, K.; Saito, T.; Ishiwata, S.; Shimakawa, Y.; Takano, M. Designed Ferromagnetic, Ferroelectric  $\text{Bi}_2\text{NiMnO}_6$ . *J. Am. Chem. Soc.* **2005**, *127*, 8889–8892.
- (19) Blasse, G. Ferromagnetic Interactions in Non-Metallic Perovskites. J. Phys. Chem. Solids 1965, 26, 1969–1971.
- (20) Dass, R. I.; Yan, J.-Q.; Goodenough, J. B. Oxygen Stoichiometry, Ferromagnetism, and Transport Properties of  $La_{2-x}NiMnO_{6+\delta}$ . *Phys. Rev. B* **2003**, *68*, No. 064415.
- (21) Kahn, O. Magnetism of Heterobimetallics: Toward Molecular-Based Magnets. In *Advances in Inorganic Chemistry*, Sykes, A. G., Ed.; Academic Press,, 1995; Vol. 43, pp 179–259.
- (22) Kahn, O.; Tola, P.; Galy, J.; Coudanne, H. Interaction between Orthogonal Magnetic Orbitals in a Copper(II)-Oxovanadium(II) Heterobinuclear Complex. J. Am. Chem. Soc. 1978, 100, 3931–3933.
- (23) Kahn, O.; Galy, J.; Journaux, Y.; Jaud, J.; Morgenstern-Badarau, I. Synthesis, Crystal Structure and Molecular Conformations, and Magnetic Properties of a Copper-Vanadyl (CuII-VOII) Heterobinuclear Complex: Interaction between Orthogonal Magnetic Orbitals. J. Am. Chem. Soc. 1982, 104, 2165–2176.
- (24) De Loth, P.; Karafiloglou, P.; Daudey, J. P.; Kahn, O. Ab Initio Calculation of the Ferromagnetic Interaction in a Copper-Vanadyl Oxide (CuIIVIIO) Heterodinuclear System. *J. Am. Chem. Soc.* 1988, 110, 5676–5680.
- (25) Gautier, R.; Oka, K.; Kihara, T.; Kumar, N.; Sundaresan, A.; Tokunaga, M.; Azuma, M.; Poeppelmeier, K. R. Spin Frustration from Cis -Edge or -Corner Sharing Metal-Centered Octahedra. *J. Am. Chem. Soc.* **2013**, *135*, 19268–19274.
- (26) Harrison, W. T. A.; Nenoff, T. M.; Gier, T. E.; Stucky, G. D. Tetrahedral-Atom 3-Ring Groupings in 1-Dimensional Inorganic Chains: Beryllium Arsenate Hydroxide Hydrate (Be<sub>2</sub>AsO<sub>4</sub>OH·4H<sub>2</sub>O) and Sodium Zinc Hydroxide Phosphate Hydrate (Na<sub>2</sub>ZnPO<sub>4</sub>OH·7H<sub>2</sub>O). *Inorg. Chem.* **1993**, *32*, 2437–2441.
- (27) Brese, N. E.; O'Keeffe, M. Bond-Valence Parameters for Solids. *Acta Crystallogr. B* **1991**, *47*, 192–197.
- (28) Kageyama, H.; Hayashi, K.; Maeda, K.; Attfield, J. P.; Hiroi, Z.; Rondinelli, J. M.; Poeppelmeier, K. R. Expanding Frontiers in Materials Chemistry and Physics with Multiple Anions. *Nat. Commun.* **2018**, *9*, No. 772.
- (29) Harada, J. K.; Charles, N.; Poeppelmeier, K. R.; Rondinelli, J. M. Heteroanionic Materials by Design: Progress Toward Targeted Properties. *Adv. Mater.* **2019**, *31*, No. 1805295.
- (30) Addison, A. W.; Rao, T. N.; Reedijk, J.; Rijn, J.; van Verschoor, G. C. Synthesis, Structure, and Spectroscopic Properties of Copper(II) Compounds Containing Nitrogen—Sulphur Donor Ligands; the Crystal and Molecular Structure of Aqua[1,7-Bis(N-Methylbenzimidazol-2'-YI)-2,6-Dithiaheptane]Copper(II) Perchlorate. J. Chem. Soc. Dalton Trans. 1984, 7, 1349—1356.
- (31) Azuma, M.; Saito, T.; Fujishiro, Y.; Hiroi, Z.; Takano, M.; Izumi, F.; Kamiyama, T.; Ikeda, T.; Narumi, Y.; Kindo, K. High-Pressure Form of  $(VO_2)P_2O_7$ : A Spin-1/2 Antiferromagnetic Alternating-Chain Compound with One Kind of Chain and a Single Spin Gap. *Phys. Rev. B* **1999**, *60*, 10145–10149.
- (32) Matsuda, M.; Kakurai, K.; Belik, A. A.; Azuma, M.; Takano, M.; Fujita, M. Magnetic Excitations from the Linear Heisenberg Antiferromagnetic Spin Trimer System A<sub>3</sub>Cu<sub>3</sub>(PO<sub>4</sub>)<sub>4</sub> (A=Ca, Sr, and Pb). *Phys. Rev. B* **2005**, *71*, No. 144411.
- (33) Hasegawa, Y.; Matsumoto, M. Magnetic Excitation in Interacting Spin Trimer Systems Investigated by Extended Spin-Wave Theory. J. Phys. Soc. Jpn. 2012, 81, No. 094712.
- (34) Hase, M.; Kohno, M.; Kitazawa, H.; Tsujii, N.; Suzuki, O.; Ozawa, K.; Kido, G.; Imai, M.; Hu, X. 1/3 Magnetization Plateau

- Observed in the Spin-1/2 Trimer Chain Compound  $Cu_3(P_2O_6OH)_2$ . *Phys. Rev. B* **2006**, 73, No. 104419.
- (35) Bencini, A.; Benelli, C.; Dei, A.; Gatteschi, D. EPR Spectra of and Exchange Interactions in Trinuclear Complexes. 3. Synthesis, Crystal Structure and Magnetic Properties of the Oxovanadium(IV) Adduct of a Tetradentate Schiff Base Copper(II) Complex. *Inorg. Chem.* 1985, 24, 695–699.
- (36) Mohanta, S.; Nanda, K. K.; Thompson, L. K.; Flörke, U.; Nag, K. Spin Exchange Coupling in Heterobimetallic MIIVIVO (M = Cu, Ni, Co, Fe, Mn) Macrocyclic Complexes. Synthesis, Structure, and Properties. *Inorg. Chem.* **1998**, *37*, 1465–1472.
- (37) Glaser, T.; Theil, H.; Liratzis, I.; Weyhermüller, T.; Bill, E. Ferromagnetic Coupling by Orthogonal Magnetic Orbitals in a Heterodinuclear CuIIVIVO Complex and in a Homodinuclear CuIICuII Complex. *Inorg. Chem.* **2006**, *45*, 4889–4891.
- (38) Baggio, R.; Contreras, D.; Moreno, Y.; Arrue, R.; Paulus, I. E.; Peña, O.; Pivan, J. Y. Magneto-Structural Study and Synthesis Optimization of a Phosphovanadate Copper Complex, [Cu-(VO)<sub>2</sub>(PO<sub>4</sub>)<sub>2</sub>·(H<sub>2</sub> O)<sub>4</sub>]<sub>n</sub>. *J. Coord. Chem.* **2012**, *65*, 2319–2331.
- (39) Manson, J. L.; A Schlueter, J.; E Garrett, K.; A Goddard, P.; Lancaster, T.; S Möller, J.; J Blundell, S.; J Steele, A.; Franke, I.; L Pratt, F.; Singleton, J.; Bendix, J.; H Lapidus, S.; Uhlarz, M.; Ayala-Valenzuela, O.; D McDonald, R.; Gurak, M.; Baines, C. Bimetallic MOFs  $(H_3O)_x[Cu(MF_6)(Pyrazine)_2]\cdot(4-x)H_2O(M=V^{4+}, x=0; M=Ga^{3+}, x=1)$ : Co-Existence of Ordered and Disordered Quantum Spins in the  $V^{4+}$  System. *Chem. Commun.* **2016**, *52*, 12653–12656.
- (40) Yucesan, G.; Yu, M. H.; Ouellette, W.; O'Connor, C. J.; Zubieta, J. Secondary Metal—Ligand Cationic Subunits {ML}<sup>n+</sup> as Structural Determinants in the Oxovanadium/Phenylphosphonate/{ML} <sup>n+</sup> System, Where {ML} Is a Cu<sup>2+</sup>/Organonitrogen Moiety. *CrystEngComm* **2005**, *7*, 480–490.
- (41) Yucesan, G.; Ouellette, W.; Golub, V.; O'Connor, C. J.; Zubieta, J. Solid State Coordination Chemistry: Temperature Dependence of the Crystal Chemistry of the Oxovanadium-Phenylphosphonate-Copper(II)-2,2'-Bipyridine System. Crystal Structures of the One-Dimensional [{Cu(Bpy)}VO<sub>2</sub>(O<sub>3</sub>PC<sub>6</sub>H<sub>5</sub>)(HO<sub>3</sub>PC<sub>6</sub>H<sub>5</sub>)], [{Cu<sub>3</sub>(Bpy)<sub>3</sub>(H<sub>2</sub>O)}V<sub>4</sub>O<sub>9</sub>(O<sub>3</sub>PC<sub>6</sub>H<sub>5</sub>)<sub>4</sub>], [{Cu-(Bpy)}<sub>2</sub>V<sub>3</sub>O<sub>6</sub>(O<sub>3</sub>PC<sub>6</sub>H<sub>5</sub>)<sub>3</sub>(HO<sub>3</sub>PC<sub>6</sub>H<sub>5</sub>)] and [{Cu(Bpy)}VO-(O<sub>3</sub>PC<sub>6</sub>H<sub>5</sub>)<sub>2</sub>]. Solid State Sci. **2005**, 7, 445–458.
- (42) Donakowski, M. D.; Gautier, R.; Yeon, J.; Moore, D. T.; Nino, J. C.; Halasyamani, P. S.; Poeppelmeier, K. R. The Role of Polar, Lamdba (Λ)-Shaped Building Units in Noncentrosymmetric Inorganic Structures. *J. Am. Chem. Soc.* **2012**, *134*, 7679–7689.
- (43) Curley, S. P. M.; Huddart, B. M.; Kamenskyi, D.; Coak, M. J.; Williams, R. C.; Ghannadzadeh, S.; Schneider, A.; Okubo, S.; Sakurai, T.; Ohta, H.; Tidey, J. P.; Graf, D.; Clark, S. J.; Blundell, S. J.; Pratt, F. L.; Telling, M. T. F.; Lancaster, T.; Manson, J. L.; Goddard, P. A. Anomalous Magnetic Exchange in a Dimerized Quantum Magnet Composed of Unlike Spin Species. *Phys. Rev. B* **2021**, *104*, No. 214435.